CrossMark

Electrochemical Reduction of X-ray Contrast Iohexol at Mixed Metal Oxide Electrodes: Process Optimization and By-product Identification

Ozge Turkay (iD) · **Sibel Barisci** · **Ebru Ulusoy** ·
Anatoly Dimoglo

Abstract The reduction of commonly used X-ray contrast iohexol (IOX) by the electrooxidation process is presented in this study. To begin with, the effect of anode material was examined, and different mixed metal oxide electrodes (MMOs) such as Ti/RuO_2, Ti/Pt, Ti/IrO_2-RuO_2, Ti/IrO_2-Ta_2O_5, Ti/Ta_2O_5-SnO_2-IrO_2, and Pt/SnO_2 were used. To assess experimental conditions at Ti/RuO_2 anode, provided the highest removal efficiency, the response surface method was applied and the key influencing parameter was the process time. The determined optimal conditions were triplicated with real wastewater samples, and the average degradation efficiency of IOX was found to be 99%. By-products of the IOX degradation on the Ti/RuO_2 anode have been identified using density functional theory and LC/MS-MS analysis. The results showed that IOX degradation opened with OH group detachment and resulted in the formation of a by-product with a molecular mass of 804 g mol^{-1}. Further degradation mechanism took place due to the breakup of C_4-C_{10} and C_5-I_7 bonds with a by-product formed as 603 g mol^{-1}. Iodide atom replacement by OH groups caused the formation of a molecular fragment with 375 g mol^{-1} molecular weight. The further disintegration of C_2-C_{11} and C_6-N_{16} σ- bonds led to the formation of molecular masses of 133, 126, and 119 g mol^{-1}, respectively.

Keywords Electrooxidation · Iohexol · Mixed metal oxides · X-ray contrast · Density functional theory · Degradation by-products

O. Turkay (✉) · E. Ulusoy
Environmental Engineering Department, Gebze Technical University, 41400 Gebze, Kocaeli, Turkey
e-mail: oturkay@gtu.edu.tr

S. Barisci
Civil and Environmental Engineering, Water and Environmental Technology (WET) Center, Temple University, Philadelphia, PA 19122, USA

A. Dimoglo
Environmental Engineering Department, Duzce University, Konuralp Campus, 81620 Duzce, Turkey

1 Introduction

The pharmaceuticals which are found in the wastewater treatment effluents have become a serious threat to the aquatic environment (Kasprzyk-Hordern et al. 2008). Although concentrations of pharmaceuticals in the surface water and wastewater are at low levels, such as micrograms per liter and nanograms per liter, they are needed to be removed from water bodies due to their adverse effects on human health and the environment. Pharmaceuticals are also usually non-biodegradable compounds (Kasprzyk-Hordern et al. 2009), and they are not amenable to conventional biological treatment due to their toxic effect on organisms even at low concentrations (Heberer 2002). Difficulties associated with conventional biological treatment of pharmaceuticals are resistance to biodegradation, toxicity to microbial cultures, and inhibition of biological treatment due to shock doses. Thus, advanced oxidation methods should be employed to remove them from waters to

avoid their potential adverse effects on humans and animals.

Advanced treatment technologies are promising for the treatment of pharmaceutical wastewater (Wols et al. 2014; Choi et al. 2014). To remove such micropollutants, electrochemical processes have become particularly attracted in the recent years (Sirés and Brillas 2012; Domínguez et al. 2012; Särkkä et al. 2015). Especially, an electrooxidation (EOX) method using mixed metal oxide (MMO) electrodes for degrading organic pollutants has attracted great interest due to its easy implementation, high efficiency, and environmental compatibility (Feng et al. 2013; Sopaj et al. 2015).

Various optimization methods have been used recently in the electrooxidation experiments to realize the effect of parameter variations on the degradation efficiency (González et al. 2011a). Generally, initial pH of the solution, applied current density, supporting electrolyte concentration, and reaction time are considered as operating variables in those studies. Among them, applied current density was found to be the most affecting factor through the electrochemical oxidation of trimethoprim (González et al. 2011a), naproxen (González et al. 2011b), and ketoprofen (Domínguez et al. 2010) with BDD anodes. The usage of experimental design also provided the determination of optimal operating conditions of the process.

Iohexol (IOX) is a commonly used pharmaceutical, and it is frequently found as iodinated contrast media in water samples. Due to its biological inertness and incomplete degradation in conventional wastewater treatment processes, IOX concentrations may reach high levels in water and groundwater samples (Wang et al. 2016). UV-based advanced oxidation techniques have been applied to the IOX removal (Giannakis et al. 2017; Pereira et al. 2007; Wang et al. 2016). The main purpose of these studies is to enhance hydroxyl radical that is

capable of degrading resistant organic substances. Ultrasound and photo-Fenton were applied, as different oxidation processes, to degrade IOX in wastewater, urine, and diluted urine samples (Papoutsakis et al. 2015). Whereas photo-Fenton process provided the complete IOX degradation, the ultrasound process was found inefficient. Electrochemical oxidation with metal oxide electrodes has drawn attentions as an alternative advanced oxidation process due to its easy implementation and low-volume requirement (Feng and Li 2003). In this study, therefore, the IOX was subjected to degradation by EOX using different electrode materials, and the most effective electrode material among MMOs was determined. In order to develop optimal conditions by using the most efficient electrode material, process optimization in this work has been conducted by response surface method (RSM). After optimum process conditions have been determined with experiments conducted using synthetic water, model verification with real wastewater was performed under optimum conditions found. Further investigation has been conducted for the IOX degradation through the determination of degradation intermediates with both analytical method and density function theory (DFT) calculations.

2 Material and Methods

2.1 Chemicals and Analytical Methods

Iohexol, namely N,N′-Bis(2,3-dihydroxypropyl)-5-(N-(2,3-dihydroxypropyl) acetamido)-2,4,6-triiodoisophthalamide ($\geq 98\%$, HPLC grade), was provided from European Pharmacopoeia. Sodium sulfate ($\geq 99.99\%$, trace metal basis) and acid/base reagents were supplied from Sigma-Aldrich. The pH of the solution was adjusted using 0.1 M H_2SO_4 and 0.1 M NaOH solutions. IOX solutions (0.5 mg L^{-1}) for the EOX

Table 1 LC/MS-MS conditions for the analysis of iohexol

Mobile phase	50% methanol, 50% ammonium formate (5 mM), 0.1% (v/v) formic acid
Flow rate	1.88–2.03 mL min^{-1}
Owen temperature	40 °C
Pressure	180 bar
Injection volume	30 μL
Analysis time	4 min

Table 2 Operating levels of the response surface quadratic model

I_d (mA cm^{-2})		pH		t (min)	
Low level (− 1)	High level (+ 1)	Low level (− 1)	High level (+ 1)	Low level (− 1)	High level (+ 1)
15	45	4	9	10	30

Fig. 1 The effect of the electrode material on the IOX degradation (experimental conditions: pH 7.1; current density of 30 mA cm^{-2}; supporting electrolyte concentration of 0.1 M of Na$_2$SO$_4$)
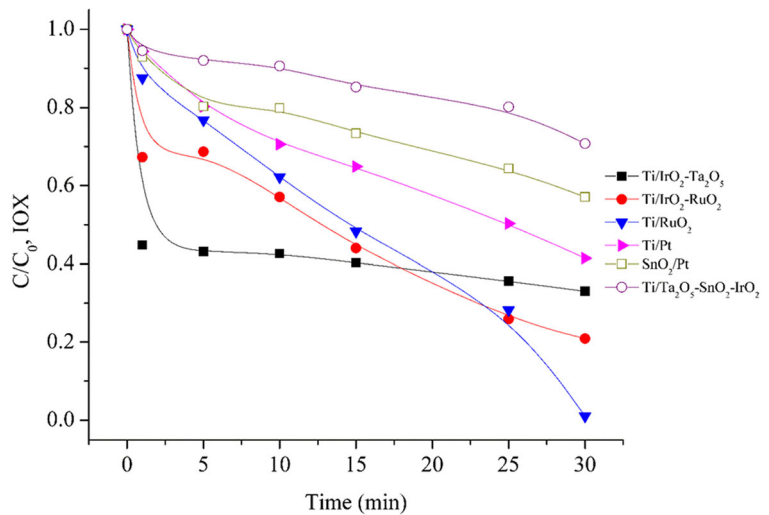
experiments were prepared daily in high-quality pure water using the Millipore Water Purification System.

Real wastewater sample was taken from a drug company, in Turkey. The initial conditions of the real wastewater were as follows: pH 7.2, conductivity 5250 μS cm^{-1}, COD 496 mg L^{-1}. The average IOX concentration was 0.525 mg L^{-1} in wastewater. The concentrations of IOX and its degradation by-products were determined via Thermo Scientific TSQ Access Max Ultimate 3000 (Triple Quadrupole) liquid chromatography-mass spectrometry (LC-MS/MS). The analytical conditions can be seen in Table 1.

2.2 Experimental Procedures

Batch experiments were carried out in an electrochemical cell with a volume of 350 mL. The anodes were MMOs (Ti/RuO$_2$, Ti/Pt, Ti/IrO$_2$-RuO$_2$, Ti/IrO$_2$-Ta$_2$O$_5$, Ti/Ta$_2$O$_5$-SnO$_2$-IrO$_2$, and Pt/SnO$_2$), where the cathodes were made of stainless steel. All the electrodes were commercially purchased from WaterDiam, France. The surface area of electrodes was 25 cm^2. Two anodes and two cathodes were placed into the electrochemical cell with a 0.5-mm gap, and then, IOX solution including 0.1 M Na$_2$SO$_4$ as supporting electrolyte was added into the cell.

Table 3 ANOVA results for the response surface quadratic model

| Source	Sum of squares	df	Mean square	F value	p value	
Model	1.22	9	0.14	7.24	0.0081	Significant
A—current density	0.25	1	0.25	13.21	0.0084	
B—pH	0.014	1	0.014	0.76	0.4109	
C—time	0.80	1	0.80	43.00	0.0003	
AB	0.017	1	0.017	0.92	0.3703	
AC	0.049	1	0.049	2.63	0.1491	
BC	1.449E−003	1	1.449E−003	0.077	0.7888	
A^2	0.010	1	0.010	0.54	0.4848	
B^2	3.552E−003	1	3.552E−003	0.19	0.6761	
C^2	0.073	1	0.073	3.93	0.0879	
Residual	0.13	7	0.019			
Lack of fit	0.13	3	0.044			
Pure error	0.000	4	0.000			
Cor total	1.35	16				

a

b
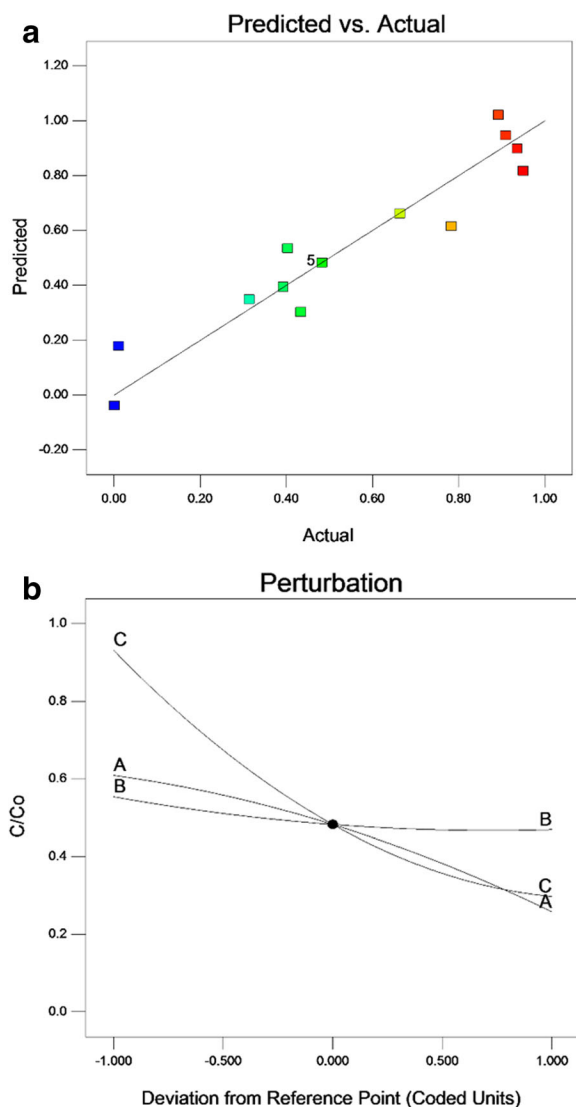
Fig. 2 **a** Relationship between the predicted and measured values for the IOX degradation efficiency at Ti/RuO₂ electrode. **b** Perturbation plot of variables (A: current density, B: pH, C: time)

The solution was stirred with a magnetic stirrer at 150 rpm during the electrolysis time. A digital power supply (0–20 A; 0–40 V) was used to provide energy during the experiments. The current density was kept constant at the levels selected as 15, 30, and 45 mA/cm^2. The experiments were performed under different pH values of the solution (4.0, 7.0 ± 02, and 9.0), to describe the pH dependence. During each run, samples were taken from the supernatant layer at different time intervals and then immediately filtered through 0.45-µm cellulose acetate membrane syringe filters (MN-

Chromafil CA-45/25) for analyses. All experiments were conducted at room temperature and duplicated.

2.3 Statistical Calculations

In the present study, Box-Behnken experimental design was set up through three selected factors (A: applied current density, B: pH, and C: process time) for the optimization of the IOX degradation of the EOX process according to the response of the IOX degradation. The removal efficiencies were fitted to a general function representing the interaction between dependent and independent variables using second-order polynomial equation. The employed model of the second order polynomial is:

$$R = \beta o + \sum \beta iXi + \sum \beta iiXi^2 + \sum \beta ijXiXj \qquad (1)$$

where R is the predicted response, Xi and Xj are independent factors, βo is the intercept, βi is the linear coefficient, βii is the quadratic coefficient, and βij is the interaction coefficient. Different levels were chosen for each parameter to determine the effect of selected parameters on the process efficiency for IOX degradation. The varieties of operating levels are summarized in Table 2. The experiments were conducted through experimental design given by RSM.

2.4 Theoretical Calculations

Model calculations were held by means of the DFT at the B3LYP ((Becke, three-parameter, Lee-Yang-Parr) [15, 16]) by taking into account parameters of salvation in aqueous environment. 6-311G++(d, p) were taken as basic functions for the calculations. As a result of the calculations, self-consistent charges on atoms, energy levels of molecular orbitals (MO), and other parameters of the electronic structure were obtained. All this made it possible to analyze the electron density distribution in IOX and to simulate the mechanism of its oxidative degradation.

3 Results and Discussion

3.1 Determination of the Electrode Material

This part of the study has been conducted to find out the most effective anode material for the IOX degradation.

Fig. 3 3D surface graph of the IOX degradation efficiency at pH 7.1
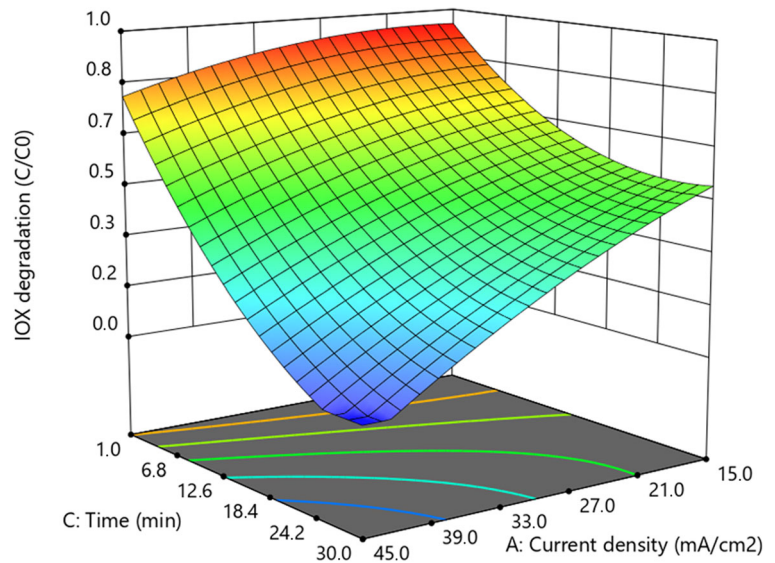
Electrooxidation tests using different MMOs, i.e., Ti/RuO$_2$, Ti/Pt, Ti/IrO$_2$-RuO$_2$, Ti/IrO$_2$-Ta$_2$O$_5$, Ti/Ta$_2$O$_5$-SnO$_2$-IrO$_2$, and Pt/SnO$_2$, were carried out under constant current density (30 mA cm^{-2}) at the original pH of the IOX solution (7.1). The effect of the anode material on the IOX degradation can be seen in Fig. 1. It can be observed that the IOX degradation efficiencies for MMO anodes noticeably differ from each other. Ti/RuO$_2$ was found as the most capable anode with 99% IOX degradation, followed by the Ti/IrO$_2$-RuO$_2$ anode with 79.1% efficiency at the end of 30-min process time. Other anodes used in the study: Ti/Pt, Ti/IrO$_2$-Ta$_2$O$_5$, Ti/Ta$_2$O$_5$-SnO$_2$-IrO$_2$, and Pt/SnO$_2$ showed poor performance on the IOX degradation as their efficiencies were in the range 29.2–67%, only. Consequently, Ti/RuO$_2$ was selected as working anode material for further experiments.

The high efficiency of the IOX degradation by Ti/RuO$_2$ anode might be contributing to its high oxygen overpotential and electrical conductivity. The highest voltage value was observed during the process with the usage of Ti/RuO$_2$, compared to other electrodes (38.2 V). In contrast, during the usage of SnO$_2$/Pt electrode, the voltage value remained in the range of 3.0–5.7 V. Besides, possible generation of free radicals may contribute high degradation efficiency. Lower efficiency for the Ti/Pt, Ti/IrO$_2$-Ta$_2$O$_5$, Ti/Ta$_2$O$_5$-SnO$_2$-IrO$_2$, and SnO$_2$/Pt was likely because of a high current leakage for oxygen evolution. Boron-doped diamond (BDD) electrode, which also has high oxygen overpotential,

provided around 90% IOX degradation with the application of 33 mA cm^{-2} of current density within 210 min of electrooxidation (Tissot et al. 2012). With the same current condition for Ti/RuO$_2$ in our experiments, the degradation efficiency of IOX was obtained as 76% at 30 min. Therefore, Ti/RuO$_2$ led to more IOX degradation efficiency than that of BDD, as well.

3.2 ANOVA Analysis and Prediction of the Model Equation

ANOVA analysis shows the significance of individual parameters and the interaction between variables. ANOVA results are presented in Table 3. As seen from Table 3, F ratio and p value of the quadratic model were obtained as 7.24 and 0.0081, respectively. According to those values, the applied model was significant. Besides, the values of "Prob > F" less than 0.0500 indicate significant model terms, and in our case, A and C (i.e., current density and process time, respectively) were significant (see Table 3). The quadratic equation obtained from regression analysis (Eq. (2)) was as follows:

$$Removal(C/C_0)$$
$$= +0.48 - 0.18A - 0.042B - 0.32C - 0.065AB - 0.11AC$$
$$+ 0.019BC - 0.049A^2 + 0.029B^2 + 0.13C^2$$

$$(2)$$

Fig. 4 **a** Overlay plot of the optimal region for the IOX degradation (the desired value for C/C_0 was selected as ≥ 0.1) and **b** experimental results for real water sample under optimized conditions
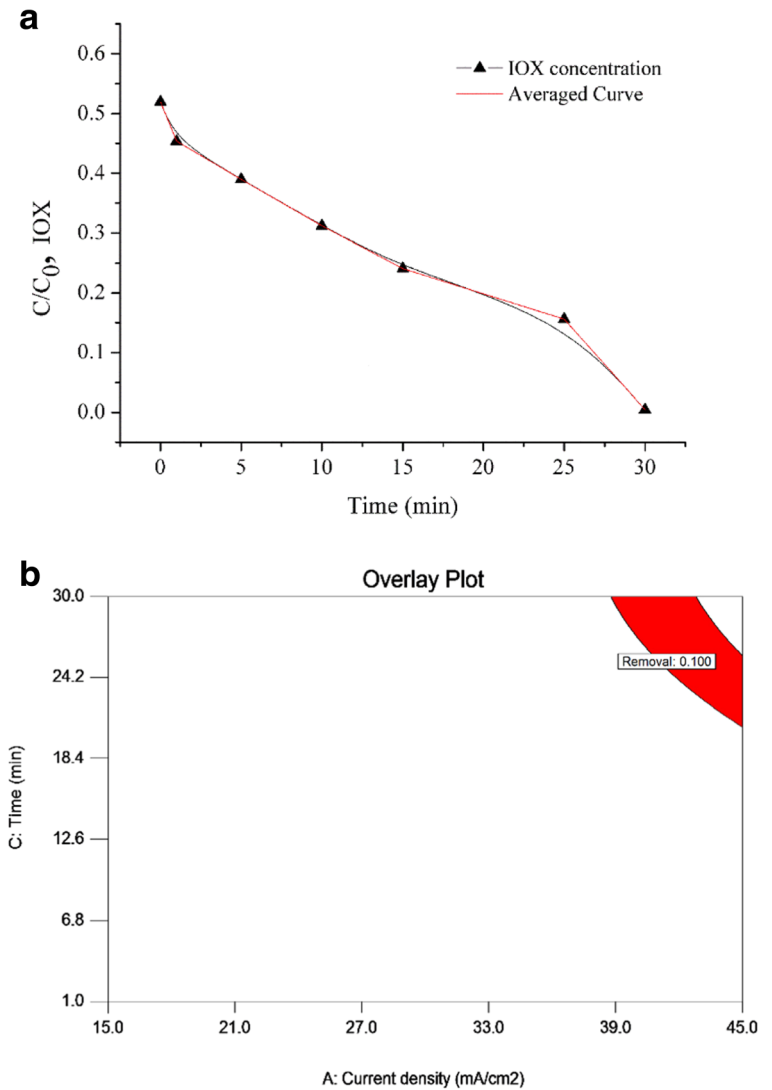
The R^2 value of the model (0.988) also suggested that the second-order polynomial model fitted the experimental results. This is confirmed by Fig. 2a, in which the plots of predicted values versus measured ones were presented. Mostly, points are distributed near the straight line that means the measured and predicted degradation efficiencies to be similar. Thus, the model is able to predict these degradation efficiencies.

Figure 2b represents the perturbation plot of variables. As seen from Fig. 2b, process time (C curve)

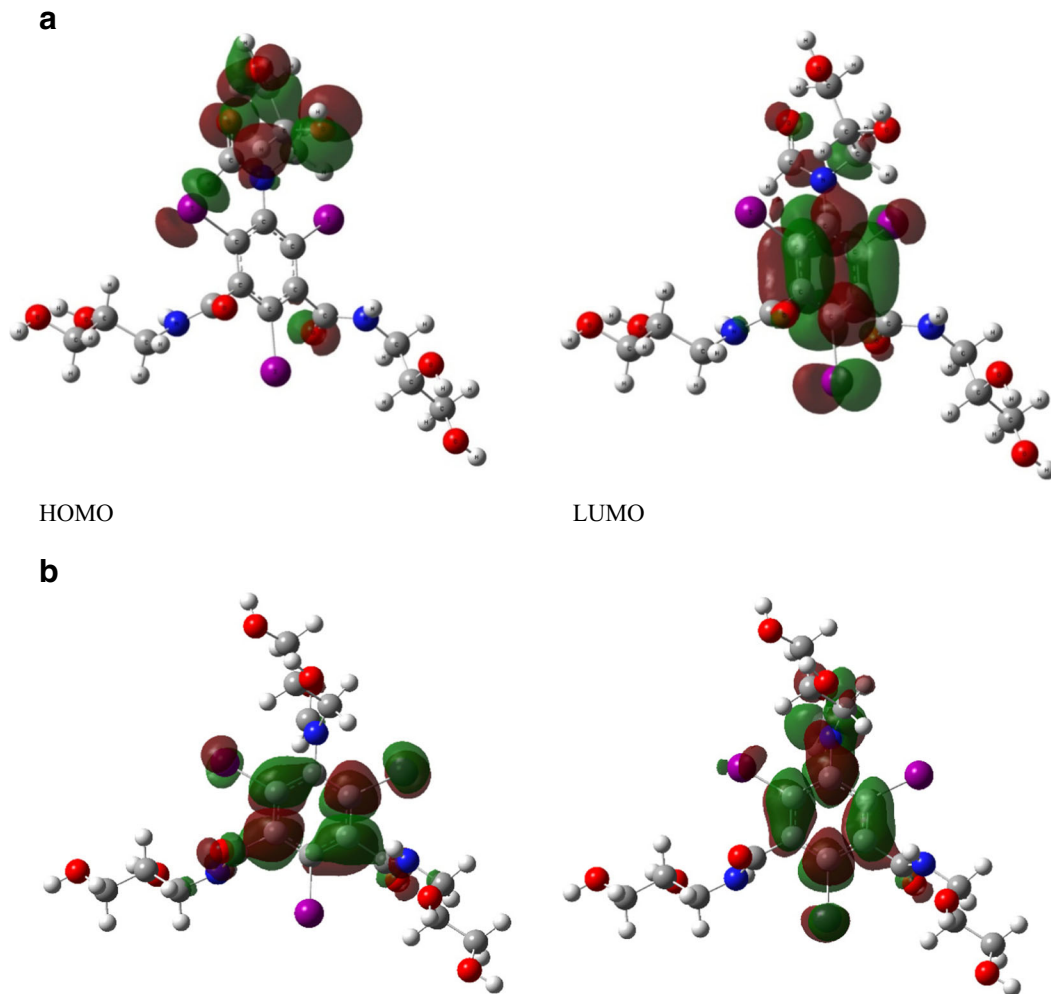Fig. 5 Density of state spectrum for the IOX (a) $q = 0$ and (b) $q = -1$

a

HOMO   LUMO

b
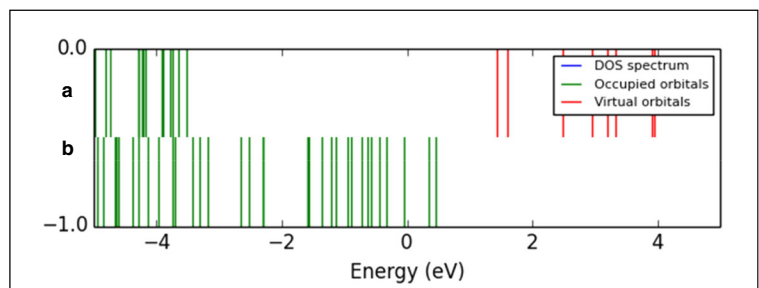
Fig. 6 The electron density distribution on the HOMO/LUMO for $q = 0$ (**a**) and $q = -1$ (**b**)

was the most effective parameter as to the IOX degradation. When process time increased to the reference point, the degradation efficiency improved. After the reference point, the efficiency showed an increasing trend, as well. Applied current density (A) also affected the IOX degradation efficiency. The increase in current density resulted in higher degradation rates. In the EOX process, applied current density is the main parameter for controlling its efficiency.

The higher applied current densities affect the anodic dissolution, and this provides greater release of hydroxyl radicals, which are able to degrade pollutants (Guinea et al. 2008; Rabaaoui and Allagui 2012). Additionally, H_2 evolution on the cathode side which increases with increasing applied current density is useful for high pollutant removal by flotation (Murugananthan et al. 2007). pH (B curve) had a negligible effect on IOX

degradation compared to the other parameters. The degradation efficiency slightly increased with increasing pH up to the reference point, and after it, a minor decrease was observed. The changes of pH did not affect the degradation efficiency during the electrochemical oxidation of pharmaceuticals (González et al. 2011a; Domínguez et al. 2010; Rabaaoui and Allagui 2012).

A 3D surface graph of the quadratic model with one of the variables kept constant and the other two ranging within the experimental conditions are shown in Fig. 3. Since the pH influence on the process efficiency was found negligible, it was kept constant at the optimal value of 7.1. Under this condition, 3D surface graph was developed by taking process time and applied current density as independent variables (see Fig. 3).

The IOX degradation efficiency was high when the applied current density and process time were

**Fig. 7** Proposed degradation pathway for the IOX according to DFT calculations
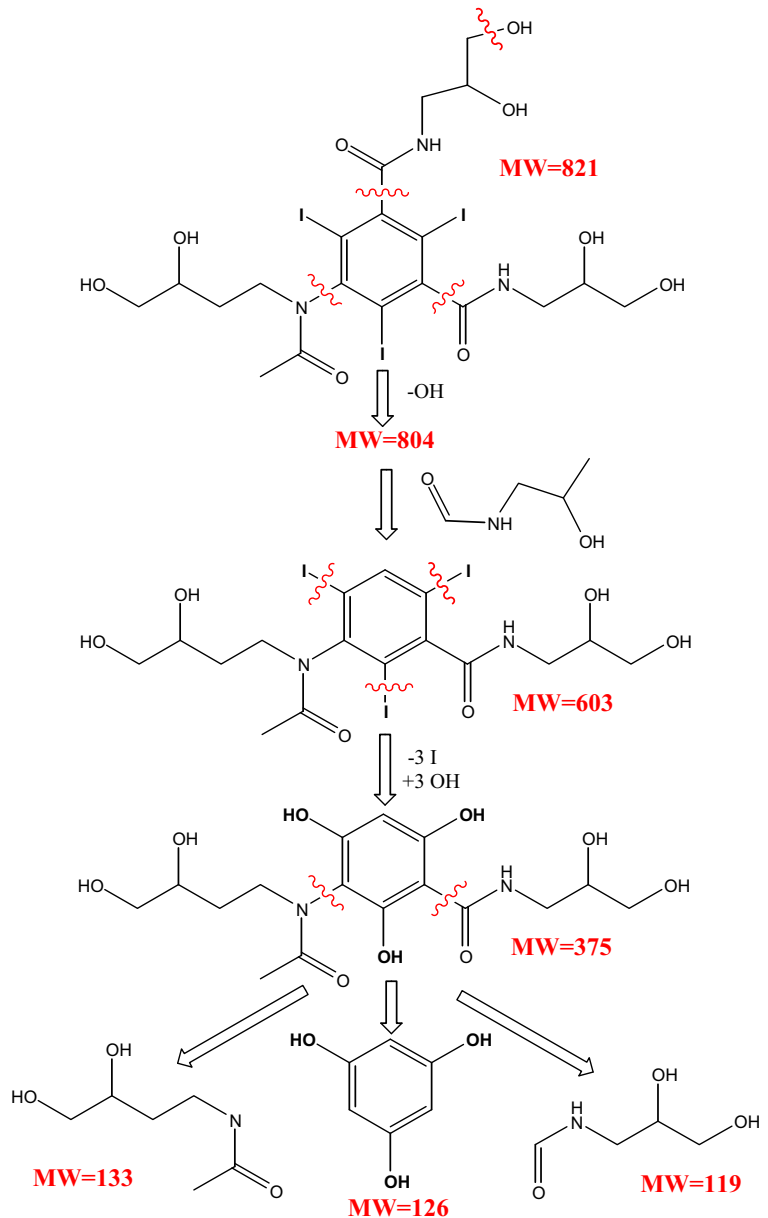
increasing within the range of 15–45 mA cm^{-2} and 0–30 min, respectively; at the optimal pH 7.1 (see Fig. 3). As it is understood from the ground curves, there was no synergistic effect when both current density and process time were lower. However, the increase in the both variability provided a higher IOX degradation efficiency. For instance, while 60% degradation efficiency was gained at the lowest applied current density (15 mA cm^{-2}), the highest applied current density (45 mA cm^{-2}) provided almost complete removal.

3.3 Optimization of Experimental Conditions of IOX Degradation and Verification of the Model

The overlay plot for the optimal region is presented in Fig. 4a. The red-shaded portion gives the allowable values of the two variables (applied current density and process time), which describe the desired limits of the IOX degradation efficiency.

When the corresponding IOX degradation efficiency was ≥ 0.1 as C/C_0, the optimal conditions calculated from the regression equation were as follows: process

Fig. 8 Identified by-products of the IOX degradation via LC/MS-MS
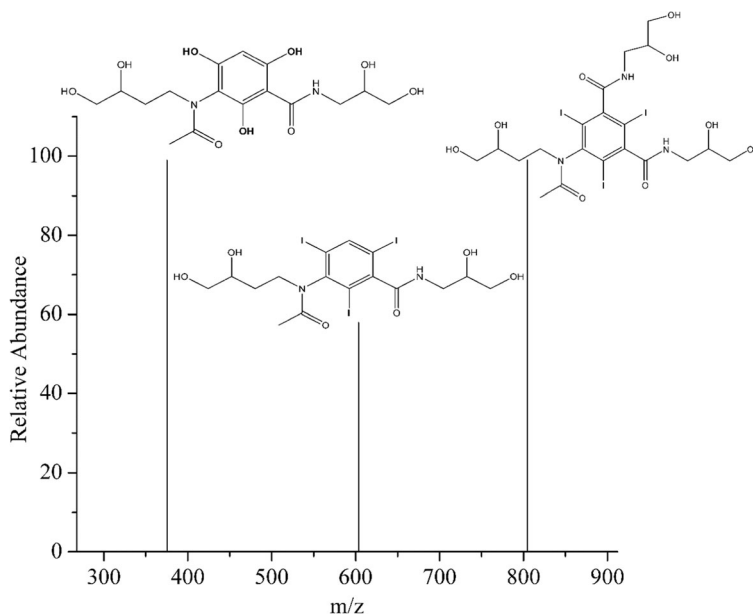
time within the range of 19.8–30 min and applied current density within the range of 38.1–45 mA cm^{-2}.

To confirm the results of the quadratic model, a confirmatory experiment under the determined optimal conditions was conducted in triplicates using real wastewater sample, and the average degradation efficiency of IOX was obtained as 99.24% (see Fig. 4b). These results were in good agreement with the predictions of the model.

3.4 Identification of By-products and Density Functional Theory Modeling

The study of the by-product identification was conducted through the density function theory supported by the results of the LC-MS-MS analysis. The search of possible products of the IOX degradation started from its electron structure calculations and those bond definitions that are capable of breaking under electrochemical impact on them. It should be emphasized that when modeling RedOx processes, the electronic state of the system itself is important. As a result of these processes, the oxidized system can take electrons from oxygen-containing particles and radicals. In this case, the attachment of an additional electron destabilizes the system due to the settlement of an anti-bonding orbitals and the weakening of the energy of individual bonds.

The calculation of the electronic structure was carried out using the Gaussian 09 program (Frisch 2004). The calculations of the effective charges on the atoms have shown that maximum negative charges are concentrated on the oxygen and nitrogen atoms, while positive charges are found on the carbon and hydrogen atoms. In Fig. 5(a, b), the changes in the state of the energy levels of the boundary orbitals in stable (a, $q = 0$) and destabilized (b, $q = -1$) states are shown. From Fig. 5(b), it is seen that the populated energy levels with the electron attachment shift to the zone of positive energy values, which leads to the destruction of the bonds entering the zone of the boundary orbitals.

Figure 6 shows that electron density on the HOMO is concentrated on the atoms of one of molecular groups, namely, -C(O)-NH-C$_2$H$_3$OH-CH$_2$OH. The orbital-acceptor (LUMO) is formed of atoms of phenyl ring and iodine atoms attached to the ring. This tells us that the changes in the electron state of a molecule consisting of the RedOx process are related to the bond destruction namely in these molecular fragments.

A similar picture was observed when the analysis of the electronic distribution on the HOMO and LUMO orbitals of the destabilized system is being the result of the RedOx process. As can be seen from Fig. 5(b), the basic electron density shifts on the bonds formed by the carbon atoms of the phenyl ring with carbon atoms and iodine atoms. From the experimental data on the LC/MS-MS study, it is seen that these bonds are primarily susceptible to weakening and rupture. A proposed pathway for the IOX degradation based on the DFT

calculations is given in Fig. 7. Accordingly, the newly formed, as the result of the IOX degradation, fragments are shown in Fig. 8. The bond C_4-C_{10} and C_5-C_{I7} breakup led to the formation of a molecular fragment with the mass 603 g mol^{-1}. The further iodide atom detachment and OH group attachment were related to the fact that the energy of these bonds, in comparison with others, was a minimal one (E_{bond} C-I = − 0.49 a.u.). The iodide atom replacement by OH groups caused the formation of the molecular fragment with molecular mass of 375 g mol^{-1} (see Fig. 8). Another further disintegration of the particle was followed by the break-up of C_2-C_{11} and C_6-N_{16} σ- bonds, which led to the formation of the molecular fragments with the massed of 133, 126, and 119 g mol^{-1}. Although no complete mineralization is achieved with the EOX process, the IOX solution became more biodegradable due to the loss of iodine from the molecule (Jeong et al. 2010). Hereby, the EOX process with a moderate applied current can be used as a pretreatment method to degrade the IOX solution.

4 Conclusions

Electrooxidation process was employed for the degradation of X-ray contrast IOX. After studying the effect of the anode material, Ti/RuO$_2$ that provided the highest degradation efficiency was selected for further tests. Response surface methodology has been applied to evaluate the experimental conditions in the usage of Ti/RuO$_2$ anode in the EOX process. The individual effect of the process time was the highest one among operating parameters. Whereas applied current density had also an effect on the IOX degradation, the pH influence was negligible. The optimal conditions calculated from the quadratic model were determined as process time within the range of 19.8–30 min and applied current density within the range of 38.1– 45 mA cm^{-2} at the optimum pH of 7.1, to get an efficiency of over 90%. In model verification, the predicted results fit with the experimental results obtained for real wastewater sample. By-products of the IOX degradation on the Ti/RuO$_2$ anode have been identified using density functional theory and LC/MS-MS analysis. The results of the theoretical calculations agreed with the experimental data. The IOX molecule degradation from 821 up to 119 g mol^{-1} was shown as a consequence of those analyses. Based on the results of the electronic structure calculations and the analysis of the electron density distribution in IOX, the mechanism of its oxidative destruction is discussed. It is shown that the transfer of an electron to the IOX molecule causes its destabilization and decay into separate fragments.

References

Choi, J., Lee, H., Choi, Y., Kim, S., Lee, S., Lee, S., et al. (2014). Heterogeneous photocatalytic treatment of pharmaceutical micropollutants: effects of wastewater effluent matrix and catalyst modifications. *Applied Catalysis B: Environmental, 147*, 8–16.

Domínguez, J. R., González, T., Palo, P., & Sánchez-Martín, J. (2010). Anodic oxidation of ketoprofen on boron-doped diamond (BDD) electrodes. Role of operative parameters. *Chemical Engineering Journal, 162*(3), 1012–1018.

Domínguez, J. R., González, T., Palo, P., Sánchez-Martín, J., Rodrigo, M., & Sáez, C. (2012). Electrochemical degradation of a real pharmaceutical effluent. *Water, Air, & Soil Pollution, 223*(5), 2685–2694.

Feng, Y., & Li, X. Y. (2003). Electro-catalytic oxidation of phenol on several metal-oxide electrodes in aqueous solution. *Water Research, 37*(10), 2399–2407.

Feng, L., van Hullebusch, E. D., Rodrigo, M. A., Esposito, G., & Oturan, M. A. (2013). Removal of residual anti-inflammatory and analgesic pharmaceuticals from aqueous systems by electrochemical advanced oxidation processes. A review. *Chemical Engineering Journal, 228*, 944–964.

Frisch, M. J., Trucks, G. W., Schlegel, H. B., Scuseria, G. E., Robb, M. A., Cheeseman, J. R., Montgomery Jr., J. A., Vreven, T., Kudin, K. N., Burant, J. C., Millam, J. M., Iyengar, S. S., Tomasi, J., Barone, V., Mennucci, B., Cossi, M., Scalmani, G., Rega, N., Petersson, G. A., Nakatsuji, H., Hada, M., Ehara, M., Toyota, K., Fukuda, R., Hasegawa, J., Ishida, M., Nakajima, T., Honda, Y., Kitao, O., Nakai, H., Klene, M., Li, X., Knox, J. E., Hratchian, H. P., Cross, J. B., Bakken, V., Adamo, C., Jaramillo, J., Gomperts, R., Stratmann, R. E., Yazyev, O., Austin, A. J., Cammi, R., Pomelli, C., Ochterski, J. W., Ayala, P. Y., Morokuma, K., Voth, G. A., Salvador, P., Dannenberg, J. J., Zakrzewski, V. G., Dapprich, S., Daniels, A. D., Strain, M. C., Farkas, O., Malick, D. K., Rabuck, A. D., Raghavachari, K., Foresman, J. B., Ortiz, J. V., Cui, Q., Baboul, A. G., Clifford, S., Cioslowski, J., Stefanov, B. B., Liu, G., Liashenko, A., Piskorz, P., Komaromi, I., Martin, R. L., Fox, D. J., Keith, T., Al-Laham, M. A., Peng, C. Y., Nanayakkara, A., Challacombe, M., Gill, P. M. W., Johnson, B., Chen, W., Wong, M. W., Gonzalez, C., & Pople, J. A. (2004). *Gaussian 03, Revision B.05*. Wallingford: Gaussian, Inc..

Giannakis, S., Jovic, M., Gasilova, N., Gelabert, M. P., Schindelholz, S., Furbringer, J.-M., et al. (2017). Iohexol degradation in wastewater and urine by UV-based advanced oxidation processes (AOPs): process modeling and by-

products identification. *Journal of Environmental Management, 195*, 174–185.

González, T., Domínguez, J. R., Palo, P., Sánchez-Martín, J., & Cuerda-Correa, E. M. (2011a). Development and optimization of the BDD-electrochemical oxidation of the antibiotic trimethoprim in aqueous solution. *Desalination, 280*(1), 197–202.

González, T., Domínguez, J. R., Palo, P., & Sánchez-Martín, J. (2011b). Conductive-diamond electrochemical advanced oxidation of naproxen in aqueous solution: optimizing the process. *Journal of Chemical Technology and Biotechnology, 86*(1), 121–127.

Guinea, E., Arias, C., Cabot, P. L., Garrido, J. A., Rodríguez, R. M., Centellas, F., et al. (2008). Mineralization of salicylic acid in acidic aqueous medium by electrochemical advanced oxidation processes using platinum and boron-doped diamond as anode and cathodically generated hydrogen peroxide. *Water Research, 42*(1), 499–511.

Heberer, T. (2002). Occurrence, fate, and removal of pharmaceutical residues in the aquatic environment: a review of recent research data. *Toxicology Letters, 131*(1), 5–17.

Jeong, J., Jung, J., Cooper, W. J., & Song, W. (2010). Degradation mechanisms and kinetic studies for the treatment of X-ray contrast media compounds by advanced oxidation/reduction processes. *Water Research, 44*(15), 4391–4398.

Kasprzyk-Hordern, B., Dinsdale, R. M., & Guwy, A. J. (2008). The occurrence of pharmaceuticals, personal care products, endocrine disruptors and illicit drugs in surface water in South Wales, UK. *Water Research, 42*(13), 3498–3518.

Kasprzyk-Hordern, B., Dinsdale, R. M., & Guwy, A. J. (2009). The removal of pharmaceuticals, personal care products, endocrine disruptors and illicit drugs during wastewater treatment and its impact on the quality of receiving waters. *Water Research, 43*(2), 363–380.

Muruganathan, M., Yoshihara, S., Rakuma, T., Uehara, N., & Shirakashi, T. (2007). Electrochemical degradation of 17β-estradiol (E2) at boron-doped diamond (Si/BDD) thin film electrode. *Electrochimica Acta, 52*(9), 3242–3249. https://doi.org/10.1016/j.electacta.2006.09.073.

Papoutsakis, S., Afshari, Z., Malato, S., & Pulgarin, C. (2015). Elimination of the iodinated contrast agent iohexol in water, wastewater and urine matrices by application of photo-Fenton and ultrasound advanced oxidation processes. *Journal of Environmental Chemical Engineering, 3*(3), 2002–2009. https://doi.org/10.1016/j.jece.2015.07.002.

Pereira, V. J., Linden, K. G., & Weinberg, H. S. (2007). Evaluation of UV irradiation for photolytic and oxidative degradation of pharmaceutical compounds in water. *Water Research, 41*(19), 4413–4423.

Rabaaoui, N., & Allagui, M. S. (2012). Anodic oxidation of salicylic acid on BDD electrode: variable effects and mechanisms of degradation. *Journal of Hazardous Materials, 243*, 187–192.

Särkkä, H., Bhatnagar, A., & Sillanpää, M. (2015). Recent developments of electro-oxidation in water treatment—a review. *Journal of Electroanalytical Chemistry, 754*, 46–56.

Sirés, I., & Brillas, E. (2012). Remediation of water pollution caused by pharmaceutical residues based on electrochemical separation and degradation technologies: a review. *Environment International, 40*, 212–229.

Sopaj, F., Rodrigo, M. A., Oturan, N., Podvorica, F. I., Pinson, J., & Oturan, M. A. (2015). Influence of the anode materials on the electrochemical oxidation efficiency. Application to oxidative degradation of the pharmaceutical amoxicillin. *Chemical Engineering Journal, 262*, 286–294.

Tissot, G. B., Anglada, A., Dimitriou-Christidis, P., Rossi, L., Arey, J. S., & Comninellis, C. (2012). Kinetic experiments of electrochemical oxidation of iohexol on BDD electrodes for wastewater treatment. *Electrochemistry Communications, 23*, 48–51. https://doi.org/10.1016/j.elecom.2012.07.006.

Wang, Z., Lin, Y.-L., Xu, B., Xia, S.-J., Zhang, T.-Y., & Gao, N.-Y. (2016). Degradation of iohexol by UV/chlorine process and formation of iodinated trihalomethanes during post-chlorination. *Chemical Engineering Journal, 283*, 1090–1096.

Wols, B., Harmsen, D., Beerendonk, E., & Hofman-Caris, C. (2014). Predicting pharmaceutical degradation by UV (LP)/H $_2$O$_2$ processes: a kinetic model. *Chemical Engineering Journal, 255*, 334–343.